LA-UR- 98-2443

Title: A Simulation of Recrystallisation Based on EBSD Orientation Microscopy Data

CONF-980964--

Author(s): Olaf Engler, CMS

MASTER

Submitted to: Riso Symposium Sept. 7-11, 1998
Roskilde, Denmark

Los Alamos
NATIONAL LABORATORY

Form No. 836 R5
ST 2629 10/91

DISCLAIMER

A SIMULATION OF RECRYSTALLISATION BASED ON EBSD ORIENTATION MICROSCOPY DATA

O. Engler

Los Alamos National Laboratory, Center for Materials Science,
K765, Los Alamos, NM 87545, USA

ABSTRACT

The present paper introduces a novel stochastic two-dimensional model to simulate the evolution of microstructure and texture during recrystallisation. The model is based on data derived by automated large-scale EBSD local texture analysis, i.e., by 'orientation microscopy'. Each measured point is characterised by its coordinates x and y in the microstructure, its crystallographic orientation g and a parameter q describing the quality of the EBSD-pattern which is affected by lattice strain and hence discloses information on the dislocation density. The concurrent information on the local arrangement of orientations and dislocation densities is utilised to derive conclusions on the nucleation and subsequent growth of the new recrystallised grains. The principles of the model are outlined and three example are shown to illustrate the possibilities of the model to simulate the evolution of microstructure and texture during recrystallisation.

1. INTRODUCTION

During annealing of a deformed metallic material recrystallisation takes place through the growth of a few subgrains of the recovered microstructure, the so-called nuclei, under consumption of their as-deformed neighbourhood. The driving force for this mechanism is provided by the energy stored in the dislocations during the deformation or, more precisely, the difference in dislocation energy between nucleus or growing grain and its surroundings. As a thermal formation of recrystallisation nuclei can be completely ruled out, the nucleation sites must pre-exist already in the as-deformed microstructure, i.e. they are an integral part of the deformed state (Doherty, 1974). However, to achieve sufficient mobility of the new grain, the nucleus must be separated by a mobile high-angle grain boundary from its neighbourhood, which means that locally misorientations of the order of 15° must exist. This restriction generally limits nucleation to regions in the vicinity of characteristic deformation heterogeneities, e.g. grain boundaries, shear bands, cube bands and large second-phase particles.

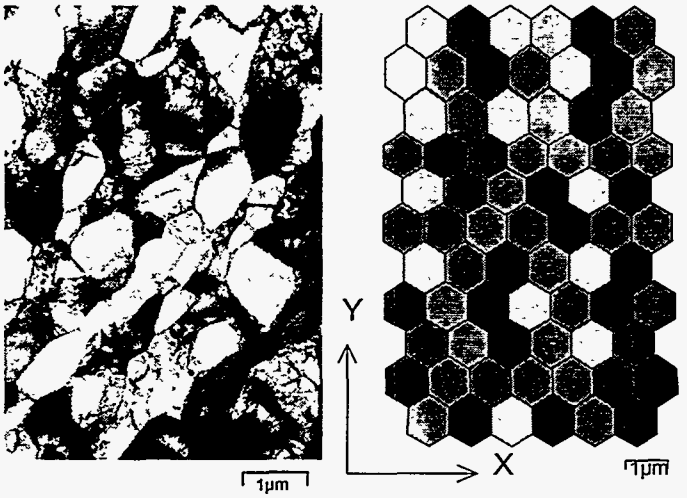

(a) recovered microstructure (Al-1.3%Mn, 90% cold rolled annealed for 20h at 350°C)

(b) schematic EBSD-orientation map as input for the model

Fig. 1. (a) Subgrain structure in recovered Al and (b) schematic orientation map of a microstructure as in (a) as input for the model.

In the present paper these mechanisms are incorporated into a stochastic two-dimensional recrystallisation model which is based on the maps derived by automated large-scale EBSD local texture analysis, i.e., by 'orientation microscopy' (Adams et al., 1993). Similarly, Baudin et al. (1997) proposed to used EBSD-orientation microscopy data as input for a Monte Carlo simulation of grain growth in Fe-3%Si transformer sheets. Provided longitudinal sections of an as-deformed or partially recrystallised sample are scanned in a sufficiently fine raster – i.e. with a step size of the order of 1µm – each measured point can be considered to be an individual subgrain of a recovered state (Fig. 1). Thus, each measured point – or subgrain in the nomenclature of the model – is characterised by its coordinates in the microstructure and its orientation which is typically given in terms of the three Euler angles φ_1, Φ, φ_2. Besides the crystallographic orientation, another parameter can be derived from the EBSD-patterns by means of image analysis, that is the sharpness or quality of the patterns. As this pattern quality q is related to the number of lattice defects, it is a measure for the strain in the lattice, which is used in the model to distinguish recrystallised grains from the cold-worked matrix (Wilkinson and Dingley, 1991, Krieger Lassen et al., 1994).

2. THE MODEL

The data for the coordinates x and y of the measured points, the orientation g and a parameter q describing the pattern quality are read from the EBSD-input file and stored in an appropriate array. Since the pattern quality is related to the number of lattice defects, it yields information about the state of deformation and internal stresses. However, besides the microstructural sample state the pattern quality is also strongly affected by the experimental set-up, so that only qualitative information can be obtained. Thus, to achieve comparable data suitable for deducing information on dislocation densities in the model, the image quality values of the deformed microstructure or the as-deformed regions in a partially recrystallised sample are scaled in the range $0<q<0.8$, whereas recrystallised regions are assigned values with $q>0.9$.

Starting with this set of input data – coordinates x and y, orientation g, image quality q and the mutual misorientations between each cell and its 6 neighbouring cells – the model is run in several time-steps (typically about 100) to yield information on the evolution of microstructure and changes in orientation distribution during progressing recrystallisation.

Recovery is characterised by the annihilation and rearrangement of dislocations into more stable configurations, i.e. in a reduction in dislocation density. In the model this is taken into account by a gradual increase in pattern quality q.

As mentioned already in the introduction, nucleation of the new recrystallised grains takes place by the growth of some specific subgrains out of the as-deformed or recovered microstructure. Accordingly, provided the corresponding characteristic nucleation sites – grain boundaries, shear bands, cube bands and large second-phase particles – are captured in the EBSD-map, nucleation is implicitly considered in the model. If required, additional nucleation sites can be introduced by arranging the nuclei and their orientations in an appropriate manner. Nucleation can occur site saturated, i.e. nuclei are formed only during the first time-step, or continuously at every time-step in the non-recrystallised volume. An example referring to particle stimulated nucleation (PSN) will be given in the next section.

Growth of the recrystallised grains is characterised by the motion of high-angle grain boundaries into the as-deformed microstructure. The driving force for this process is provided by the annihilation of dislocations, and thus the reduction in dislocation energy, in the affected microstructure regions. In the model this is considered as follows: For each cell the misorientations with regard to the 6 neighbouring cells is determined. If a mobile high-angle grain boundary is encountered – indicated by a misorientation angle exceeding 15° – the probability of growth into this neighbouring cell is derived by the difference in pattern quality between the two cells, multiplied with a random number. If the resulting value exceeds a given threshold value, the considered cell grows into the neighbouring cell, which means that the orientation g and pattern quality q of the latter are replaced with the data of the growing grain. This ensures that the growth probability of a recrystallised grain characterised by a high q into the as-deformed neighbourhood is quite large (Fig. 2a). However, this also means that deformed cells with higher pattern quality (i.e. low dislocation energy) may be able to grow on the expense of neighbouring subgrains with poorer pattern quality (Fig. 2b). Thus, a subgrain on one side of a pre-existing high-angle grain boundary can grow into subgrains with higher dislocation densities (poorer image quality) on the other side, a mechanism which is commonly referred to as strain-induced boundary migration (SIBM; Doherty, 1974).

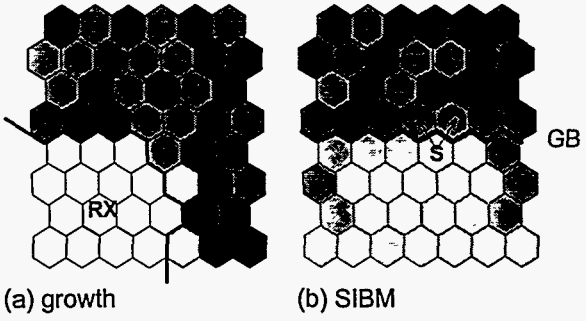

Fig. 2. Schematic representation of (a) growth of a recrystallised grain *RX* into the as-deformed neighbourhood and (b) strain induced boundary migration of a subgrain *S* across a high-angle grain boundary *GB*.

After each time-step the misorientation data are updated and the new microstructure is plotted on the computer screen. The resulting macrotexture can be determined by calculating the orientation distribution function (ODF) from the orientations of the individual cells or, if desired, only from the recrystallised cells. The microstructure can be output in a data format which enables one to create and plot orientation maps according to the options of the post-processing software used. The maps shown in this paper are produced with the software package OIM 2.5 by TexSEM Labs., Inc. The individual cells are either shaded according to their image quality q, or to a colour scheme characteristic of the orientation of the corresponding cell. Low-angle grain boundaries with misorientation angles between 3° and 15° and high-angle grain boundaries with misorientation angles exceeding 15° are respectively marked with thin and thick lines. The recrystallised volume fraction can readily be derived from the ratio between recrystallised and non-recrystallised cells. The final grain size of the recrystallised grains D_{RX} can be estimated from the number of recrystallisation nuclei.

3. APPLICATIONS

To illustrate the possibilities of the model to account for the evolution of microstructure and texture during recrystallisation for a variety of different materials and conditions, the model was applied to different cases, and three of them will be addressed in the following.

The first example pertains to the evolution of the well-known cube-recrystallisation texture in cold rolled copper. A 2000x2000μm^2 sampling area of a partially recrystallised 95% cold rolled Cu-sheet with a recrystallised volume fraction of about 10% was scanned in 20μm steps by means of EBSD (Necker et al., 1997); Fig. 3a shows the resulting orientation map, shaded in terms of the image quality q. Evidently, the microstructure consists of a large portion of as-deformed regions with a large fraction of high-angle grain boundaries (which is caused by the quite coarse step size) as well as a few large contiguous cube-oriented regions, the so-called cube-bands (e.g. Doherty et al., 1995). During the subsequent growth period these cube-regions continue to grow under consumption of the as-deformed microstructure. Additionally, nuclei

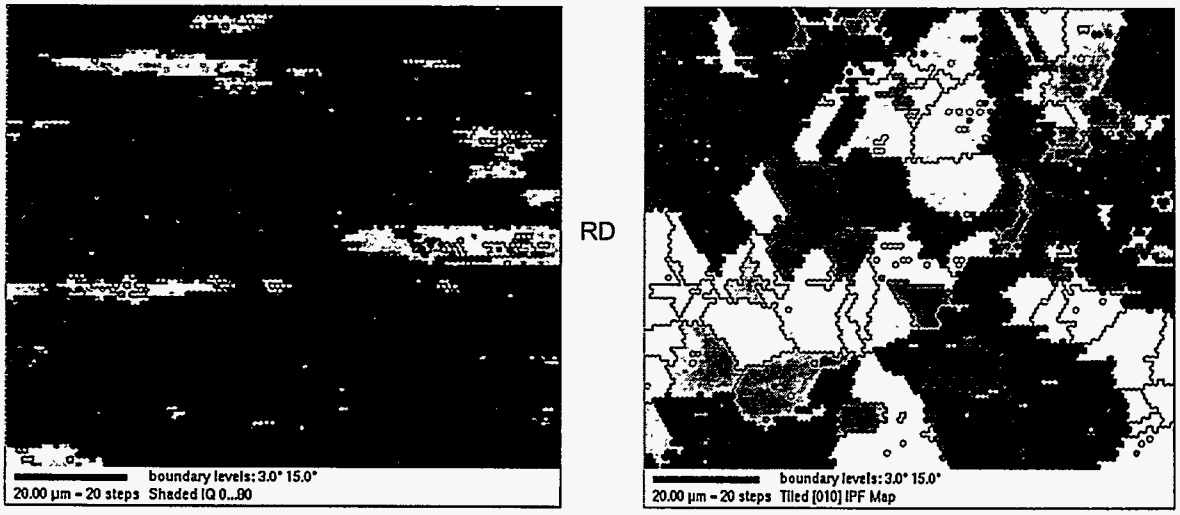

(a) initial state (partially recrystallised, $X(t)\approx10\%$) (b) recrystallised structure

Fig. 3. Simulation of the recrystallisation in Cu.

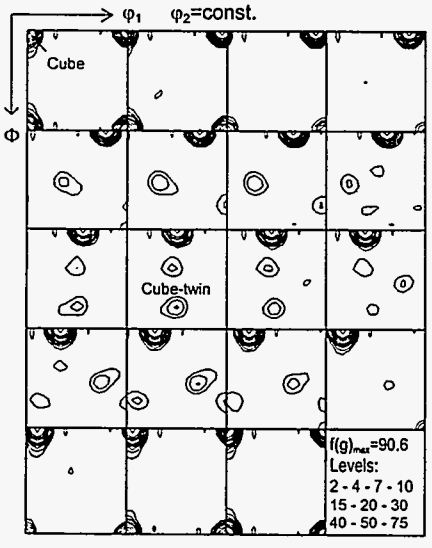

Fig. 4. ODF of the orientation map in Fig. 3b.

were observed to form at other sites in the microstructure, e.g. at high-angle grain boundaries, and then to grow until eventually the entire microstructure was comprised of quite coarse recrystallised grains (Fig. 3b). The texture of the initial state, i.e. the partially recrystallised sample, comprised the typical rolling texture components C={112}<111>, S={123}<634> and B={011}<211> as well as the cube-orientation {001}<100> with some scatter about the rolling direction. After complete recrystallisation the texture is much sharper, $f(g)_{max}\approx90$, and merely consists of the cube-orientation and its twins (Fig. 4). Note that in the model code no twinning has been introduced so far, which means that the cube-twins must exist already in the partially recrystallised state. Because of favourable conditions with regard to image quality and local misorientation, such regions can grow to noticeable components during the model calculations.

In the next example, the model was applied to an orientation map of a coarse grained Al-3%Mg sample which was cold rolled to 90% thickness reduction and recovery annealed for 3s at 400°C. The recrystallisation texture of this material consists of a strong cube-orientation and some intensities of the R-orientation {124}<211>, whose nuclei can be attributed to the existing high-angle grain boundaries, and the Q-orientation {013}<231> which can be tracked down to nucleate at shear bands (Engler, 1996).
The map of the initial state consists of a heavily banded as-deformed microstructure with some traces of shear bands (arrowed in Fig. 5a). During the first time-steps of the model calculations a large number of nuclei formed at the high-angle grain boundaries and the shear bands in the microstructure. Fig. 5b shows the modelled orientation map after complete recrystallisation, which comprises a rather non-uniform grain size distribution. The recrystallisation texture determined from this map shows strong rolling-texture orientations including the R-orientation, a strong peak of the Q-component as well as minor intensities of the cube- and Goss-orienta-

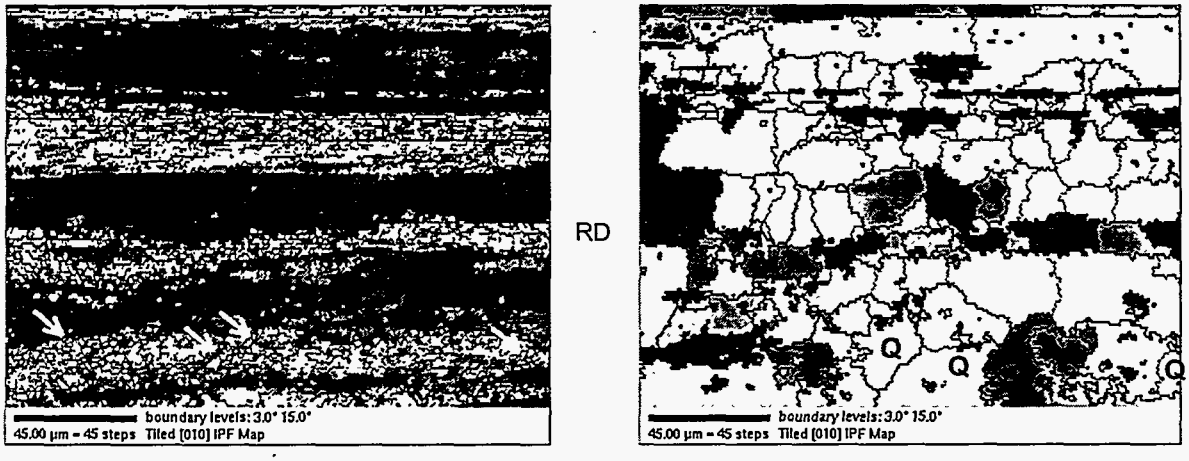

(a) initial state (recovered) (b) recrystallised structure

Fig. 5. Simulation of the recrystallisation in Al-3%Mg.

tions (Fig. 6). It turned out that the recrystallised grains with rolling texture orientations were elongated parallel to the former rolling direction RD which can be attributed to their nucleation at the pre-existing high-angle grain boundaries. Q-oriented grains appeared to be clustered in the vicinity of the former shear bands of the as-deformed state (Fig. 5b), which confirms that this orientation is caused by nucleation at the shear bands (Engler, 1996). The texture results qualitatively resembled the corresponding experimental recrystallisation texture, though the ratio between the various recrystallisation texture components strongly differed. For instance, the cube-orientation is much weaker that in the experimental texture, which means that the volume of cube-bands recorded was too small indicating that the statistics in the present map was not sufficient.

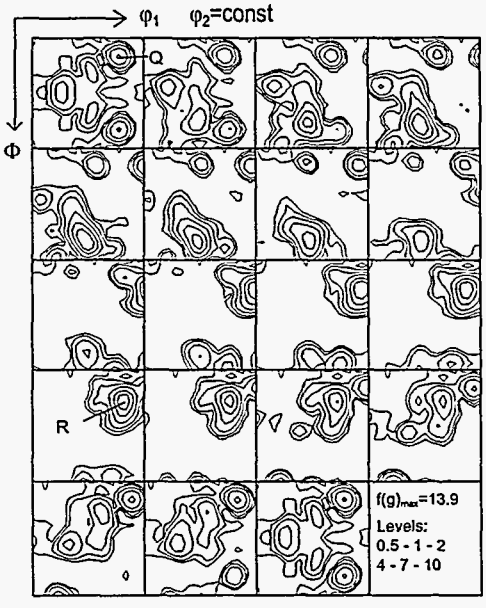

Fig. 6. ODF of the orientation map in Fig. 5b.

In the last example the nucleation at large second-phase particles will be addressed, which is a very important nucleation mechanism in many commercial aluminium alloys (e.g. Ørsund and Nes, 1988, Vatne et al., 1997). Particle stimulated nucleation (PSN) takes place in the turbulent zones that form during deformation around large particles to accommodate deformation incompatibilities (Humphreys, 1977). However, scanning of these extremely fine deformation zones by means of EBSD would require a very fine raster with step size of about 0.1µm which is of the same order as the spatial resolution of the EBSD-technique. Hence, an accurate detection of the subgrain orientations in the deformation zones is doubtful, especially in the highly cold-worked samples where PSN is of particular importance. Furthermore, such a fine raster results in very large data sets that have to be acquired and processed to provide orientation maps with statistical relevance. In order to overcome these difficulties, in the present case PSN-nuclei were 'artificially' introduced by exchanging the orientation and increasing the pattern quality of an appropriate number of cells (~6%) chosen in a random manner. In order to take the 40°<111> microgrowth selection of successful PSN-nuclei into account (Engler et al., 1996), the original

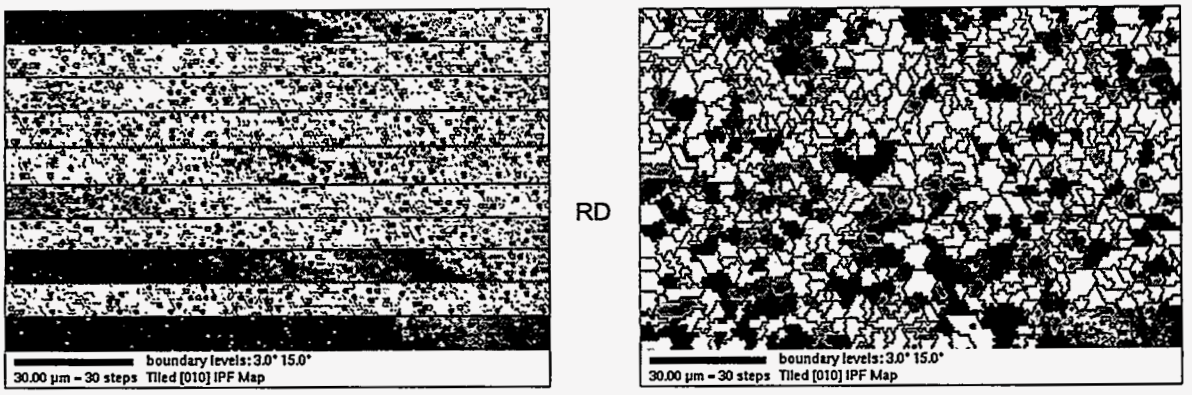

(a) initial state (PSN) (b) recrystallised structure

Fig. 7. Simulation of the recrystallisation in the case of PSN.

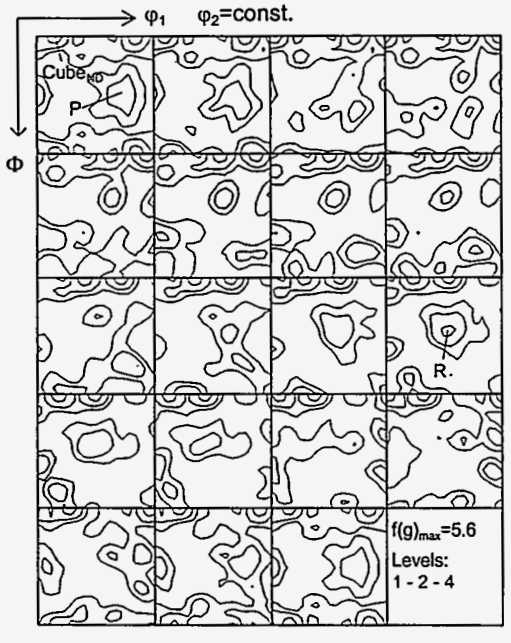

Fig. 8. ODF of the orientation map in Fig. 7b.

orientation was rotated by an angle of approximately 40° about an axis close to one of the eight possible <111>-axes. PSN is commonly considered to be site-saturated, so that the corresponding subroutine in the code was activated only once during the first time-step.

Fig. 7a shows an orientation map of a computer-generated deformed microstructure just after the occurrence of PSN, and Fig. 7b the corresponding map after complete recrystallisation. As expected, the introduction of a large number of additional nucleation sites leads to a very fine grained microstructure and a quite weak recrystallisation texture (Fig. 8) in comparison to the examples obtained in the absence of particles. Because of the introduction of nuclei with a 40°<111> orientation relationship to the deformed matrix, the recrystallisation texture corresponds to a 40°<111> transformed rolling texture which is characterised by a cube-orientation being significantly rotated

about the normal direction towards {001}<310> and a weak P-component {011}<122> (Engler, 1997). This is in very good agreement with experimental recrystallisation textures of samples where nucleation is dominated by PSN (Engler, 1996, Vatne et al., 1997).

4. SUMMARY AND CONCLUSIONS

The present paper introduces a novel stochastic recrystallisation model that, starting from the orientation maps derived by automated large-scale EBSD local texture analysis, i.e., by orientation microscopy, simulates the evolution of microstructure and texture with progressing recrystallisation. The model is based on two major assumptions: (i) Growth can only take place if the growing (sub)grain is separated from its surroundings by a mobile high-angle grain boundary. This means that a given cell must have a misorientation exceeding 15° to its neighbouring cell under consideration. (ii) The driving force for recrystallisation is provided by the difference in stored energy between two neighbouring cells. In the model this is taken into account by considering the difference in pattern quality q of the two cells. Despite the low number of basic assumptions – which are very well established in the literature – the microstructure simulated by the model appears to be very realistic with regard to grain size and shape, and the simulated recrystallisation textures contain the most important features of the recrystallisation textures of similar samples observed experimentally.

It turned out that the main limitation of the model was caused by the lack in availability of accurate orientation maps of as-deformed microstructures, which need to be obtained with sufficient spatial resolution (steps of about 1μm) and sufficient statistical relevance (scans of minimum 100x100, better 200x200 or more measured points).

Interestingly, the simulations proved to be much more accurate if the model was applied to 'real' orientation maps, i.e. maps determined experimentally, rather than 'synthetic' maps generated in the computer. This reflects the fact that the as-deformed microstructure is much more complex than one would usually take into account when generating an orientation map, and nucleation of recrystallisation just starts in such heavily disturbed regions of the microstructure.

In conclusion, starting from an orientation map obtained by EBSD orientation microscopy in a deformed or partially recrystallised sample, the model is able to simulate the evolution of the microstructure during recrystallisation in a reasonable way and furthermore predicts meaningful data for recrystallised grain size and recrystallisation texture. Thus, besides its illustrative and didactic character, the model is very well suited for an estimate of the evolution of microstructure and texture during a recrystallisation anneal of the given sample. Furthermore, with an appropriate set of boundary conditions, the model is able to yield information about the impact of variations in certain microstructure features on the recrystallisation behaviour.

ACKNOWLEDGEMENTS

This work has been supported by the U.S. Department of Energy and by the Alexander von Humboldt-Foundation through a Feodor Lynen Research Fellowship. The author is grateful to Dr. U.F. Kocks for valuable discussions. Thanks are also due to Dr. C.T. Necker for providing the orientation maps of the partially recrystallised copper.

REFERENCES

Adams, B.L., Wright, S.I., and Kunze, K., (1993). Orientation Imaging: the Emergence of a New Microscopy. Met. Trans. 24A, 819-831.

Baudin, T., Paillard, P., and Penelle, R. (1997). Grain Growth Simulation Starting from Experimental Data. Scripta mater. 36, 789-794.

Doherty, R.D. (1974). The Deformed State and Nucleation of Recrystallization. Metal Sci. 8, 132-142.

Doherty, R.D., Samajdar, I., Necker, C.T., Vatne, H.E., and Nes, E. (1995). Nucleation of Recrystallization in Cold and Hot Deformed Polycrystals. In: Microstructural and Crystallographic Aspects of Recrystallization, Proc. 16th Risø Int. Symp. on Materials Science. Edited by N. Hansen, D. Juul Jensen, Y.L. Liu, and B. Ralph (Risø Nat. Lab, Roskilde, Denmark) 1-23.

Engler, O. (1996). Nucleation and Growth during Recrystallisation of Aluminium Alloys Investigated by Local Texture Analysis. Mat. Sci. Tech. 12, 859-872.

Engler, O. (1997). Simulation of the Recrystallization Textures of Al-Alloys on the Basis of Nucleation and Growth Probability of the Various Textures Components. Textures and Microstructures 28, 197-209.

Engler, O., Yang, P., and Kong, X.W. (1996). On the Formation of Recrystallization Textures in Binary Al-1.3%Mn Investigated by Means of Local Texture Analysis. Acta mater. 44, 3349-3369.

Humphreys, F.J. (1977). Nucleation of Recrystallization at Second Phase Particles in Deformed Aluminium. Acta metall. 25, 1323-1344.

Krieger Lassen, N.C., Juul Jensen, D., and Conradsen, K. (1994). Automatic Recognition of Deformed and Recrystallized Regions in Partially Recrystallized Samples Using Electron Back Scattering Patterns. Mat. Sci. Forum 157-162, 149-158.

Ørsund, R., and Nes, E. (1988). Effect of Particles on Recrystallization Textures in Al-Mn Alloys. Scripta Metall. 22, 665-669.

Necker, C.T., Doherty, R.D., and Rollett, A.D. (1997). Development of Recrystallization Texture and Microstructure in Cold Rolled Copper. In: Proc. of ReX '96, the 3rd Int. Conf. on Recrystallization and Related Phenomena. Edited by T.R. McNelley (Monterey Institute of Advanced Studies, Monterey, CA) A1-A8.

Vatne, H.E., Engler, O., and Nes, E. (1997). The Influence of Particles on the Recrystallisation Textures and Microstructures of Aluminium Alloy AA3103. Mat. Sci. Technol. 13, 93-102.

Wilkinson, A.J., and Dingley, D.J. (1991). Quantitative Deformation Studies Using Electron Back-Scatter Patterns. Acta metall. mater. 39, 3047-3055.